2017 International Conference on
Unmanned Aircraft Systems (ICUAS)
June 13-16, 2017, Miami, FL, USA

Towards the Development of an Autonomous Interdiction Capability for Unmanned Aerial Systems

Hongze Alex See, Satadal Ghosh, and Oleg Yakimenko

Abstract — **As well-known, interdiction operations in adversarial environments can be quite challenging. With the advancement in technologies and applications involving unmanned aerial systems, an efficient autonomous aerial interdiction mission has been identified in literature as one of the pivotal elements. Effective interdiction usually requires a group of pursuers (as opposed to a single one), which enables achieving a certain formation around the target restricting its further maneuver. This paper presents a coordinated trajectory-shaping guidance strategy for a group of two autonomous pursuers, which can easily be generalized for a multi-pursuer case. Specific challenges in the group maneuvering include coordinated control of the arrival time and final relative attitude. The paper develops the corresponding algorithms and demonstrates their effectiveness in a set of computer simulations featuring different engagement geometries. It also addresses feasibility of obtained solutions from the standpoint of their applicability on board of a small unmanned aerial vehicle with a limited computational capability.**

IV. INTRODUCTION

Unmanned aerial systems (UASs) have a great potential to provide diverse capabilities to conduct missions across the wide range of military operations: environmental sensing and battlespace awareness; weapon detection and counter-weapon capabilities; port security; precision targeting; and precision strike [1]. Furthermore, the capabilities provided by these unmanned systems continue to expand. The vision of the U.S. Department of Defense (DoD) for unmanned systems is the seamless integration of diverse unmanned capabilities that provide flexible options for operators while exploiting the inherent advantages of unmanned technologies, including persistence, size, speed, maneuverability, and reduced risk to human life. DoD envisions unmanned systems teaming with manned systems (MUM) while gradually reducing the degree of human control and decision making required for the unmanned portion of the force structure [1]. MUM missions include cargo, air refueling, interdiction in contested areas, electronic/network attack, suppression of enemy air defenses, and other traditional air combat missions [1].

Hongze Alex See is with the Department of Systems Engineering, Naval Postgraduate School, Monterey, CA 93943, USA (phone: +1 (831) 915-0130, e-mail: hsee@nps.edu).

Satadal Ghosh is a U.S. National Research Council Research Associate at the Department of Systems Engineering, Naval Postgraduate School, Monterey, CA 93943, USA. This research was performed while Satadal Ghosh held an NRC Research Associateship award at the Naval Postgraduate School. (e-mail: sghosh@nps.edu).

Oleg A. Yakimenko is with the Department of Systems Engineering and Department of Mechanical and Aerospace Engineering, Naval Postgraduate School, Monterey, CA 93943, USA (e-mail: oayakime@nps.edu).

With the ever growing threats of piracy, attacks, and weapons proliferation from the adversaries in contested the airspace, there is an increasing need to interdict a suspect/intruder successfully to ensure safety and protection of such unmanned systems. This could be mechanized by deploying some of the armed unmanned aerial vehicles (UAVs) to engage and interdict targets independently or cooperatively with other systems.

This paper deals with such an interdiction mission, where the use of autonomous swarming UAVs could offer new unique capabilities. The successful use of a Control Architecture for Robotic Agent Command and Sensing (CARACaS) in unmanned surface vehicles for overwhelming adversaries has firmly paved the path in this direction for unmanned systems in general [2]. In order to achieve a successful air interdiction mission this paper proposes a swarming concept in which a group of armed pursuer UAVs is required to achieve a desired coordinated formation relative to the target UAV's position and heading simultaneously, which assures successful containing and/or intercepting the target. To this end, a coordinated trajectory-shaping guidance strategy is developed for a group of autonomous pursuers rather than for an individual pursuer. While this paper considers only the case of a two-pursuer interdiction mission the developed algorithms could easily be extended to a general case of multi-pursuer interdiction mission.

The problems of controlling final time (a.k.a. impact time) and terminal angle (a.k.a. impact angle) in an engagement have been dealt with mainly in the guidance-related literature. Impact-angle-constrained engagement problems have extensively been studied using optimal control theory [3]-[9], sliding mode control theory [10]-[12], proportional navigation (PN)-based methodology [13]-[17], and other nonlinear methods like relative circular navigation [18]. The problem of controlling impact time has also been addressed in literature using the optimal control theory [19], [20], PN-based strategy [21], [22], and sliding mode control theory [23]. With the few exceptions ([6], [20], [23]) these two problems have usually been dealt with independently. However, as mentioned earlier, for a successful interdiction mission controlling both the arrival attitude and arrival time needs to be achieved simultaneously. That is exactly what the current paper concentrates on.

Dealing with aforementioned problem the optimal-control-theory-based methods heavily rely on linearized engagement geometry. These methods exhibit a significant sensitivity to time-to-go estimation errors. Sliding-mode-control-based methods and strategies based on proportional navigation (PN) have the potential to explore the problems considering their nonlinearity. However, the advantage of

978-1-5090-4494-8/17/$31.00 ©2017 IEEE

PN-based methods lies in the simple but elegant and efficient user-friendly structure of a guidance command. This paper presents a novel real-time-implementable guidance strategy for a group of pursuers based on PN guidance philosophy to simultaneously approach the locations sufficiently close to a moving target while maintaining a desired terminal heading. Specifically, a simple adaptive variation of the navigation gain for one of pursuers in the group is shown to be effective for a successful interdiction mission in general.

The paper is organized as follows. Section II formulates the problem of interdiction mission that involves multiple pursuers. Section III formalizes a procedure for assuring coordinated trajectory-shaping guidance for the group of two autonomous pursuers, followed by Section IV discussing the results of a couple of representative computer simulations. Section V concludes the paper presenting a plan of implementation of the developed algorithms on board of a small UAV.

II. Multi-Pursuer Interdiction Problem Formulation

A. Basic Engagement Configuration

This paper considers a planar engagement when pursuers are relatively close to each other but could have different speeds and headings (Fig. 1). Pursuers are assumed to be homogeneous with typically a comparable or slight advantage over the target's speed. The target is assumed to be non-maneuvering but moving with a constant speed and heading. The target is also assumed to adopt a flee-away strategy instead of engaging in a close combat and attempting to out-maneuver pursuers. Relying on its speed therefore becomes a priority for the target. Pursuers are assumed to be equipped with sensors allowing them to detect and track the target's location and heading relative to the pursuers. The problem of decision-making for each individual pursuer to determine its own respective position in the formation is out of the scope of this paper. Thus, assuming that the intercept point (IP) and approach angle for each pursuer in the formation are pre-determined by a centralized mission controller. Figure 1 shows an example of engagement configuration with the final desired configuration achieved when all pursuers arrive on the circle around the target with the pre-defined headings simultaneously.

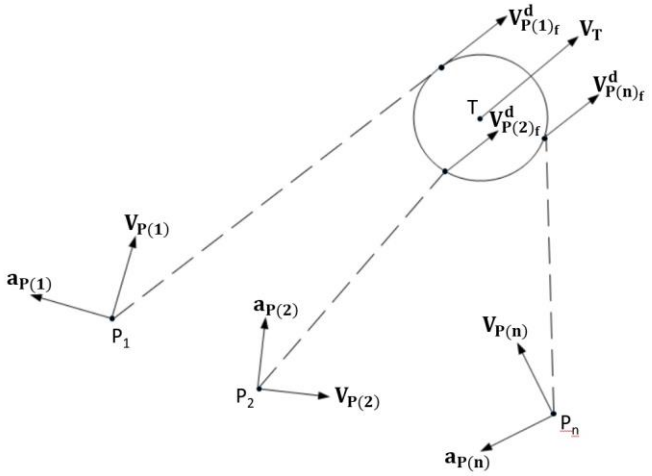

Figure 1. Planar engagement geometry.

In accordance with the planar engagement geometry depicted in Fig.1, each pursuer P is modeled as a point mass moving with constant speed $V_P = \|\mathbf{V}_P\|$ approaching a stationary target T. As a result, kinematic equations of motion for two components of the speed vector, V_R and V_θ, respectively, are expressed in terms of the range between P and T, R, and corresponding line-of-sight (LoS) angle, θ, as

$$V_{R(i)} = \dot{R}_{(i)} = -V_{P(i)}\cos(\alpha_{p(i)} - \theta_{(i)}) \quad (1)$$

$$V_{\theta(i)} = R_{(i)}\dot{\theta}_{(i)} = -V_{P(i)}\sin(\alpha_{p(i)} - \theta_{(i)}) \quad (2)$$

In these equations, 'i' represents the i-th pursuer, and the change of the pursuer's velocity heading angle α_p is defined by its lateral acceleration $a_P = \|\boldsymbol{a}_P\|$ ($\boldsymbol{a}_P$ is orthogonal to the speed vector since we consider the case when V_P = const)

$$\dot{\boldsymbol{\alpha}}_{\boldsymbol{P(i)}} = \boldsymbol{a}_{\boldsymbol{P(i)}}/V_{P(i)} \quad (3)$$

Pursuer's lateral acceleration a_P is based on the Pure Proportional Navigation (PPN) guidance law with the given by

$$a_{P(i)} = V_{P(i)}\dot{\alpha}_{P(i)} = N_{(i)}V_{P(i)}\dot{\theta}_{(i)} \quad (4)$$

where N is the navigation gain.

The problem of having a moving target, as opposed to a stationary target considered in [24], is dealt with by estimating Predicted IP (PIP). Other than that, the approach angle control is carried in a similar manner, using the so-called approach angle-constrained guidance laws against a stationary target [24] allowing approaching the target from any direction (i.e., $\alpha_{P_f} \in [-\pi, \pi)$).

B. Background of PN-Based Approach Angle Control

From Eqs. (3) and (4), the achievable approach angle using the standard PPN guidance is given by

$$\alpha_{P_f} = \alpha_{P_0} + N(\theta_f - \theta_0) \quad (5)$$

in the case of $\alpha_{P_0} \geq \theta_0$, i.e., $\alpha_{P_0} \in [\theta_0, \theta_0 + \pi)$.

The collision course with a stationary target (PIP in our case) is formed when $\alpha_{P_f} = \theta_f$ [25]. From Eq.(5) it follows that:

$$\alpha_{P_f} = (N\theta_0 - \alpha_{P_0})/(N-1) \quad (6)$$

If the condition for the bounded terminal lateral acceleration of pursuer is met ($N \geq 2$), the achievable approach angle interval using PPN becomes [26]

$$\alpha_{P_f} \in \left[2\theta_0 - \alpha_{P_0}, \theta_0\right), \quad N \geq 2 \quad (7)$$

where α_{P_f} equals $2\theta_0 - \alpha_{P_0}$ when N = 2, and approaches θ_0 when $N \to \infty$. It could also be noted that using the standard PPN, a significant portion of the angular interval in the halfspace $[-\pi + \theta_0, \theta_0)$ cannot be achieved since $\left[2\theta_0 - \alpha_{P_0}, \theta_0\right) \subset [-\pi + \theta_0, \theta_0)$. A two-stage PPN guidance strategy (2pPPN) introduced in [14] expanded the set of the achievable approach angles. Specifically, the following theorem established the achievable approach angle set and corresponding navigation gains for PPN and 2pPPN ([19], [24]):

Theorem 1. In the case of $\alpha_{P_0} > \theta_0$, a desired approach angle $\alpha_{P_f}^d \in [2\theta_0 - \alpha_{P_0}, \theta_0)$ could be attained using PPN with $N = (\alpha_{P_f}^d - \alpha_P)/(\alpha_{P_f}^d - \theta) \geq 2$, while $\alpha_{P_f}^d \in [-\pi + \theta_0, 2\theta_0 - \alpha_{P_0})$ could be achieved using 2pPPN with

$$N = \begin{Bmatrix} \left(\frac{2}{\pi}\right)\{\alpha_{P_0} - \theta_0\} & if\ (\alpha_{P_f}^d - \alpha_P)/(\alpha_{P_f}^d - \theta) < 2 \\ (\alpha_{P_f}^d - \alpha_P)/(\alpha_{P_f}^d - \theta) & if\ (\alpha_{P_f}^d - \alpha_P)/(\alpha_{P_f}^d - \theta) \geq 2 \end{Bmatrix} \quad (8)$$

Figure 2 presents examples of trajectories utilizing PPN and 2pPPN for $\alpha_{P_f}^d = -\pi/6$, and $\alpha_{P_f}^d = -5\pi/6$, respectively, with and without the look-angle ($\mu = \alpha_P - \theta$) constraint. It should be noted that the initial range between the pursuer and target should be sufficiently large and is determined by the initial LoS rate, maximum turn rate of pursuer, pursuer's speed, and desired terminal angle. Following a similar methodology for $\alpha_{P_0} \in (-\pi + \theta_0, \theta_0)$ Theorem 1 can be restated as the following observation:

Observation 1. In the case of $\alpha_{P_0} < \theta_0$, a desired approach angle $\alpha_{P_f}^d \in (\theta_0, 2\theta_0 - \alpha_{P_0}]$ could be attained using PPN with $N = (\alpha_{P_f}^d - \alpha_P)/(\alpha_{P_f}^d - \theta) \geq 2$, while $\alpha_{P_f}^d \in (2\theta_0 - \alpha_{P_0}, \pi + \theta_0]$ could be achieved using 2pPPN with

$$N = \begin{Bmatrix} \left(\frac{2}{\pi}\right)|\alpha_{P_0} - \theta_0| & if\ (\alpha_{P_f}^d - \alpha_P)/(\alpha_{P_f}^d - \theta) < 2 \\ (\alpha_{P_f}^d - \alpha_P)/(\alpha_{P_f}^d - \theta) & if\ (\alpha_{P_f}^d - \alpha_P)/(\alpha_{P_f}^d - \theta) \geq 2 \end{Bmatrix} \quad (9)$$

Since for two specific initial conditions (collision course $\alpha_{P_0} = \theta_0$ and inverse collision course $\alpha_{P_0} = -\pi + \theta_0$) algorithm cannot start, use of an adjustment bias was suggested in [24].

The approach angle control considered in this paper is an extension over the results in Theorem 1 and Observation 1 stated above to accommodate the requirement of simultaneous arrival of pursuers at the desired final intercept points relative to now moving target.

C. Background of PN-based Final Time Control

As mentioned above, a PIP needs to be computed with respect to the target's estimated position and heading. For that, time-to-go should be computed for each pursuer in the group. A closed-form time-to-go estimate for the stationary targets is given by

$$\hat{t}_{go} = \begin{Bmatrix} \left(\frac{R}{V_P}\right)\left\{1 + \frac{\theta_P^2}{[2(2N-3)]}\right\} & if\ N > \frac{3}{2} \\ \left(\frac{R}{V_P}\right)\left[1 - 2\theta_P^2\left\{1 - \frac{\left[\ln\left(\frac{R}{R_{min}}\right)\right]}{4}\right\}\right] & if\ N = \frac{3}{2} \end{Bmatrix} \quad (10)$$

where $R_{\min}$ represents the minimum range for an intercept to occur. More details of this result can be found in [27]. This approximate form of time-to-go is dependent on instantaneous range R, angle between pursuer heading and LoS θ_P (a.k.a. heading error with respect to the target), navigation gain N and pursuer's speed.

As PIPs are computed for all pursuers, and corresponding time-to-go estimates are obtained, this information could be utilized for adaptive variation of navigation gain of some of the pursuers. Next section specifically addresses strategies and algorithms for a two-pursuer intercept model.

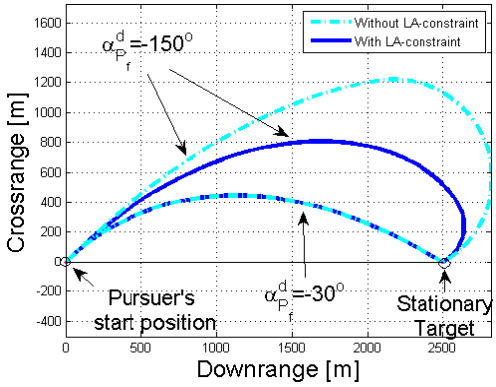

Figure 2. Examples of pursuer trajectory for PPN and 2pPPN.

III. STRATEGIES FOR INTERDICTION MISSION

A. PIP Estimation for Each Pursuer

The first step to achieve simultaneous arrival time for all pursuers is to estimate the time-to-go for each pursuer to their respective PIP, $\hat{t}_{go(i)}$. The algorithm to estimate the time-to-go for each control cycle is as follows:

1. Initialization step (at the start of every control cycle)

a) Obtain information about the current range $R_{mag(i)} = \|\mathbf{R}_{mag(i)}\|$ from the target, velocity $V_{P(i)}$ and current heading $\alpha_{P(i)}$ for Pursuers 1 and 2, together with the speed of the target $V_T = \|\mathbf{V}_T\|$ and target's current heading, α_T.

b) Guess the time-to-go $t_{guess(i)}$ for each pursuer

$$t_{guess(i)} = \frac{1}{2}\left(\frac{R_{mag(i)}}{V_{P(i)} - V_T} + \frac{R_{mag(i)}}{V_{P(i)} + V_T}\right) \quad (11)$$

2. Recursion step (within a control cycle).

Follow this step while the difference between $t_{guess(i)}$ and $\hat{t}_{go(i)}$ is less then 5%, i.e. $t_{guess(i)} \geq 1.05\hat{t}_{go(i)}$ or $t_{guess(i)} \leq 0.95\hat{t}_{go(i)}$. Otherwise, go to Step 3.

a) Use $t_{guess(i)}$ to compute the coordinates of the guessed PIP $\hat{\mathbf{R}}_{guess(i)}$ from the guessed time-to-go value, $t_{guess(i)}$, with the current desired PIP $\mathbf{R}(i)$ for each individual pursuer

$$\hat{\mathbf{R}}_{guess(i)} = \mathbf{R}(i) + \mathbf{V}_T t_{guess(i)} \quad (12)$$

b) Obtain the LoS angle $\theta_{guess(i)}$ for Pursuers 1 and 2 with respect to (w.r.t.) guessed PIP, to compute the required navigation gain for each pursuer

$$N_{(i)} = (\alpha_T - \alpha_{P(i)})/(\alpha_T - \theta_{guess(i)}) \quad (13)$$

c) Following (10) evaluate the time-to-go estimate $\hat{t}_{go(i)}$ for each pursuer with parameters $\hat{R}_{guess(i)} = \|\hat{\mathbf{R}}_{guess(i)}\|$, $V_{P(i)}$, $\theta_{P(i)} = \alpha_{P(i)} - \theta_{guess(i)}$ and $N_{(i)}$.

d) Increase or decrease the guessed time-to-go $t_{guess(i)}$ with a half the difference between $t_{guess(i)}$ and time-to-go estimate $\hat{t}_{go(i)}$

$$t_{guess(i)} = t_{guess(i)} + (\hat{t}_{go(i)} - t_{guess(i)})/2 \quad (14)$$

3. Exit step. The time-to-go estimate for each pursuer $\hat{t}_{go(i)}$ to the PIP is obtained for the control cycle. And, the PIP, LoS angle and gain for the control cycle is obtained as,

$$\boldsymbol{R}_{PIP(i)} = \boldsymbol{R}(i) + \boldsymbol{V}_T\hat{t}_{go(i)};\ \theta_{(i)} = \theta_{guess(i)};$$
$$N_{(i)} = (\alpha_T - \alpha_{P(i)})/(\alpha_T - \theta_{(i)}) \quad (15)$$

B. *Trajectory-Shaping Strategy for Multiple Pursuers*

In the guidance generation, the moving target is computed as a stationary target in every computational cycle (a.k.a. control cycle). Therefore, the overall guidance algorithm could be adopted from Theorem 1 and Observation 1, where a proportional navigation-based guidance law is proposed for capturing all possible impact angles in a surface-to-surface planar engagement against a stationary target.

Following Theorem 1 and Observation 1, angle control is achieved. However, to implement final time control, a further adaptive modulation of navigation gain is required which is discussed next.

According to Eq.(10), in order to enable a synchronized arrival of all pursuers they should adjust either their speed profiles or navigation gains. Reducing the navigation gain of pursuer with a lower time-to-go to a value less than 2, allows the pursuer to fly a longer trajectory and acts as a kind of an extra roaming phase for the corresponding pursuer. The navigation gain value greater than or equal to 1 also ensures that the target and PIP are still within its field of view. A computational procedure for the two-pursuer case looks like follows:

1) Initialization step. The time-to-go estimates, $\hat{t}_{go(1)}$ and $\hat{t}_{go(2)}$, and corresponding navigation gains, $N_{(1)}$ and $N_{(2)}$, at each control cycle for Pursuers 1 and 2 are obtained from Step 3 of PIP estimation algorithm in Section IIA.

2) If $(|\hat{t}_{go(1)} - \hat{t}_{go(2)}| \leq \underline{t}_{go_{th}})$, the navigation gains $N_{(1)}$ and $N_{(2)}$ for Pursuers 1 and 2 remain unchanged.

3) Recursive step (over control cycles). While $(|\hat{t}_{go(1)} - \hat{t}_{go(2)}| \geq \underline{t}_{go_{th}})$, set $N_{(1)}$=1 if $\hat{t}_{go(2)} > \hat{t}_{go(1)}$ or $N_{(2)}$=1 if $\hat{t}_{go(1)} > \hat{t}_{go(2)}$. Compute the new positions for the next control cycle of Pursuers 1 and 2 with $N_{(1)}$ and $N_{(2)}$, respectively, and thus for the next control cycle $\hat{t}_{go(1)}$ and $\hat{t}_{go(2)}$ till $(|\hat{t}_{go(1)} - \hat{t}_{go(2)}| \leq \underline{t}_{go_{th}})$. Go to Step 4.

4) Recursive step (over control cycles). While $(|\theta_{(1)} - \alpha_T| \geq \pi/12)$ re-initiate gain scheduling for pursuer 1 by setting $N_{(1)}$ = 1 if $(\hat{t}_{go(2)} - \hat{t}_{go(1)} \geq \overline{t}_{go_{th}})$, and while $(|\theta_{(2)} - \alpha_T| \geq \pi/12)$ re-initiate gain scheduling for pursuer 2 by setting $N_{(2)}$ = 1 if $(\hat{t}_{go(1)} - \hat{t}_{go(2)} \geq \overline{t}_{go_{th}})$. For each successive control cycle repeat this gain scheduling for pursuer 1 until $(|\theta_{(1)} - \alpha_T| < \pi/12)$ or $(|\hat{t}_{go(1)} - \hat{t}_{go(2)}| \leq \underline{t}_{go_{th}})$, and for pursuer 2 until $(|\theta_{(2)} - \alpha_T| < \pi/12)$ or $(|\hat{t}_{go(1)} - \hat{t}_{go(2)}| \leq \underline{t}_{go_{th}})$.

5) Recursive step (over control cycles). Otherwise use $N_{(1)}$ and $N_{(2)}$ computed from Step 3 of PIP estimation algorithm in Section IIA until pursuers arrive at their corresponding PIPs.

In this paper, the threshold of $\overline{t}_{go_{th}} = 3$s has been considered as different from the threshold of $\underline{t}_{go_{th}} = 1$s used in Step 2 and Step 3. In Steps 2 and 3, an attempt is made to bring Pursuers 1 and 2 to arrive simultaneously within the considered threshold $\underline{t}_{go_{th}} = 1$s for the first time. Following this, no gain scheduling is performed and the positions of the pursuers are computed along with the computed $N_{(1)}$ and $N_{(2)}$. During this time the difference in $\hat{t}_{go(i)}$ is likely to grow. Attempts to reduce the difference in $\hat{t}_{go(i)}$ are made again when the difference grew to the threshold of $\overline{t}_{go_{th}} = 3$s.

IV. SIMULATION RESULTS

This section presents and discusses the results of two simulations characterizing two different intercept scenarios. In all simulations the integration step (a.k.a control cycle) was 0.05*s* (corresponding to the 20-Hz update rate). All simulations were executed on an Intel Core i7 2.20 GHz computer with 8.00 GB RAM in the MATLAB development environment.

The simulations have the following similar engagement parameters: initial coordinates of Pursuer 1 $\mathbf{R}_{P1}$=[0,0]^{T}m , initial coordinates of Pursuer 2 $\mathbf{R}_{P2}$=[0,0]^{T}m, initial coordinates of non-maneuvering moving target $\boldsymbol{R}_T$ = [2500, -1000]^{T}m, final desired angle of Pursuer 1 intercept point with respect to target's heading $\theta_{P1\text{-}T}$ = π/4, final desired angle of Pursuer 2 intercept point with respect to target's heading $\theta_{P2\text{-}T}$ = -3π/4, final desired range of Pursuer 1 intercept point from target $R_{P1\text{-}T}$ = 100m and final desired range of Pursuer 2 intercept point from target $R_{P2\text{-}T}$ = 100m. The two pursuers in each simulation will have a different initial heading. The two pursuers in different simulations may have either the same or different speeds. For simulation with same velocity magnitude, the initial velocity vector of Pursuer 1 $\mathbf{V}_{P1}$=50*[cos(2π/3), sin(2π/3)]^{T}m/s and the initial velocity vector of Pursuer 2 $\mathbf{V}_{P2}$=50*[cos(3π/4),sin(3π/4)]^{T}m/s. For simulation with different speed magnitudes, the initial velocity vector of Pursuer 1 $\mathbf{V}_{P1}$=[-35, 25]^{T}m/s and the initial velocity vector of Pursuer 2 $\mathbf{V}_{P2}$ =[-40, 30]^{T}m/s.

To begin with, Figs. 3 and 4 present trajectories of two pursuers approaching a stationary target. The idea is to demonstrate / reiterate that simulations involving non-maneuvering target are a product of considering the target to be stationary at every computational cycle.

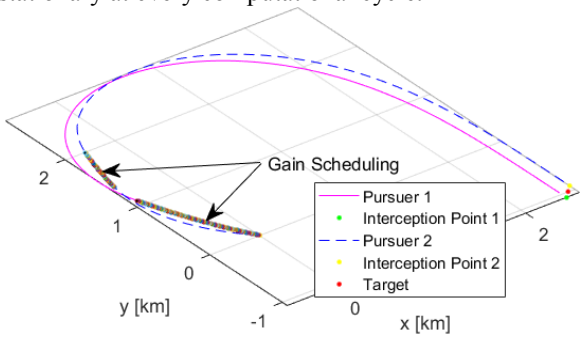

Figure 3. Trajectory of two pursuers with similar velocity magnitude to a stationary target.

Figure 5 demonstrates the convergence of the approach simultaneously with the time histories of the navigation gain of pursuers, time histories of the range between pursuers and the intercept points and the angle between pursuers and LoS, respectively. In Figs. 3,4 and 6, the control cycle that a pursuer has been assigned the navigation gain value of 1 is marked in black and labeled 'gain scheduling'.

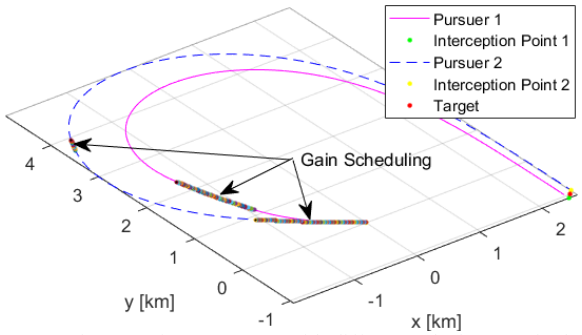

Figure 4. Trajectory of two pursuers with different velocity magnitude to a stationary target.

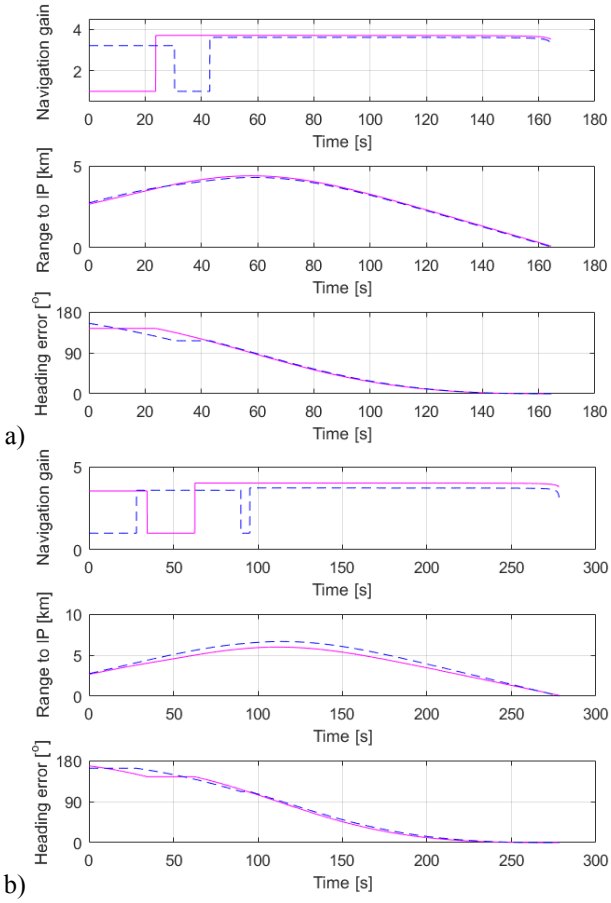

Figure 5. Navigation gain, time histories of the range between pursuers and intercept points and angle between pursuers' heading for trajectories shown in Figs. 3 and 4, respectively.

Figs. 6 and 7 present simulation results similar to that of Figs. 3-5 with the exception of a non-maneuvering moving target instead of a stationary target.

The range to the intercept point graphs in Figs. 6 and 7 demonstrate the concept of simultaneous approach with the convergence of the pursuers at their respective intercept points at the end of the guidance computation. While the aim of the guidance strategy is set up to achieve pin-point simultaneous approach for both pursuers, it is noticed that the ranges of both pursuers did not fully converged. This can be seen more clearly in the range to intercept graph in Fig. 7c, where Pursuer 1 (represented by the pink line) has yet to arrive at its intercept point. This observation is expected and will vary with different threshold limits stated in Section II.

It can also be observed in Figs. 3, 4 and 6 that the pursuer that is scheduled a navigation gain value of 1 took a longer path at that particular section while the corresponding pursuer caught up, seen in navigation gain graphs and the range to intercept point graphs in Figs. 5 and 7.

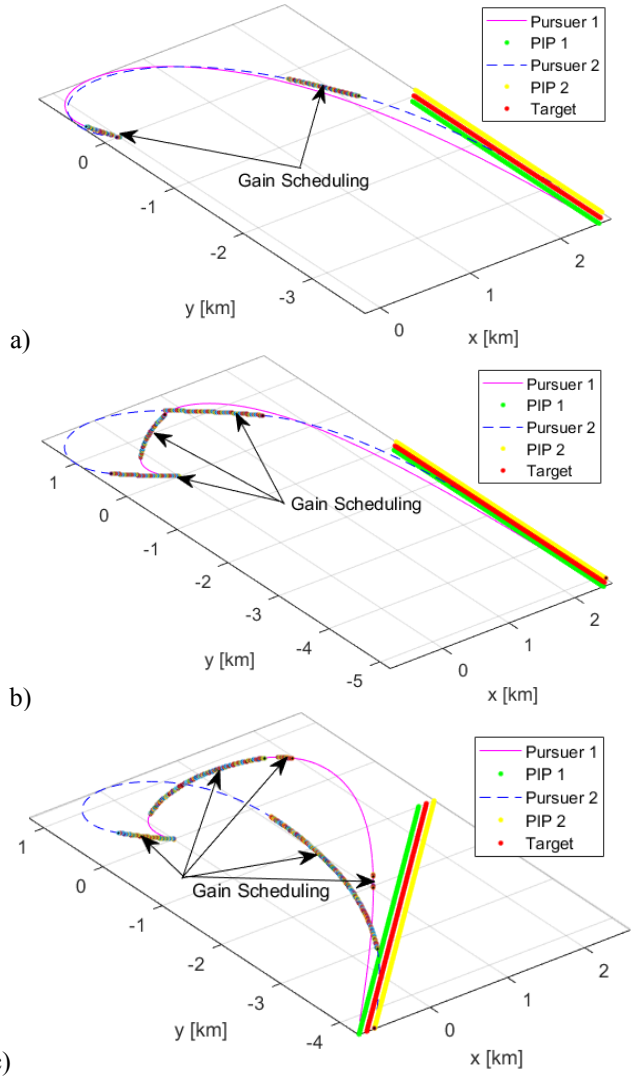

Figure 6. Trajectories of two pursuers with similar velocity magnitude (a) and trajectories of the two pursuers with different velocity magnitude (b) to a non-maneuvering target with velocity vector $\mathbf{V}_T$ = [0; -20]^{T}m/s and trajectories of the two pursuers with similar velocity magnitude (c) to a non-maneuvering target with velocity vector $\mathbf{V}_T$ = [-20; -20]^{T}m/s.

The time history of the heading error with respect to the target shown in Figs. 5 and 7, demonstrates that the angle between the pursuers' heading and LoS and demonstrate the angle-constrained approach where the heading errors of the pursuers converged to zero (aligned with the LoS) at the end of the guidance computation. In this simulation, it was pre-determined that the final desired pursuers' headings will be similar to the target's heading.

In the simulation, we have used serial computation for PIP and time-to-go estimation. Even with serial computation, the guidance generation is < 3% which is much less than guidance command interval. The total guidance computation time with its respective mission time for each simulation is

presented in Table 1. In practice, the UAVs with onboard computational payload would imply parallel computation and the computational burden would not pose any significant adverse effect. This implies that algorithm can be run in real-time implementation [24].

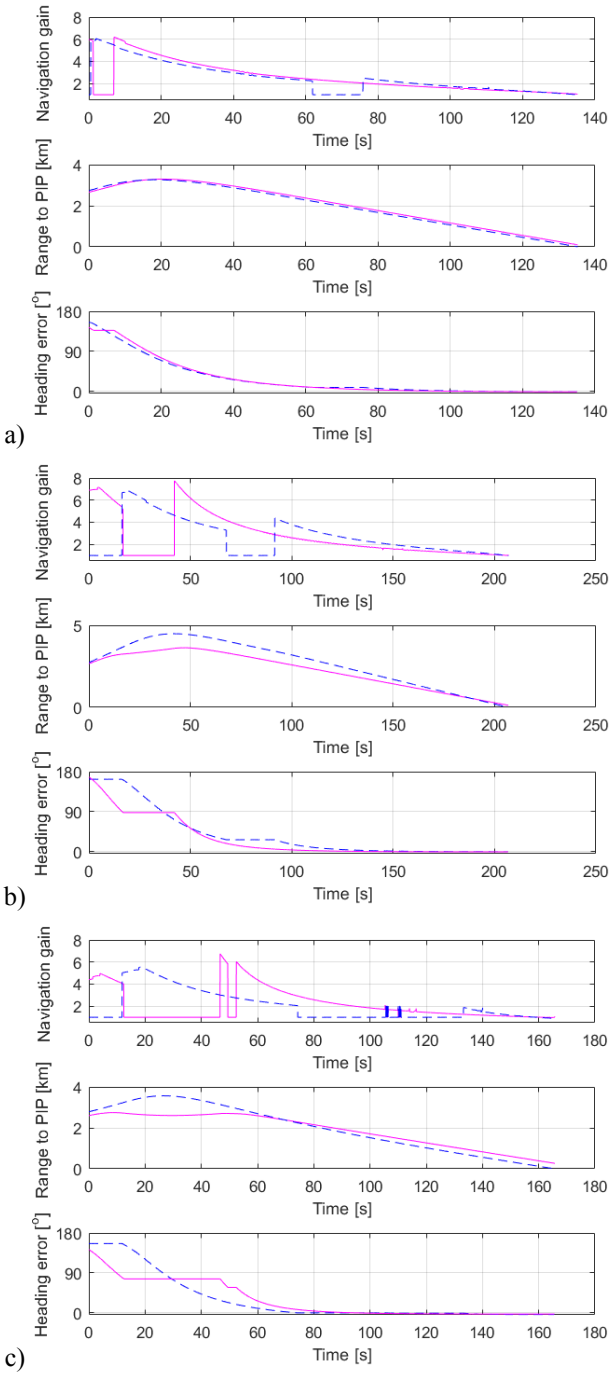

Figure 7. Navigation gain, time histories of the range between the pursuers and PIPs and angle between pursuers' heading for trajectories shown in Figs. 6a, 6b and 6c, respectively.

Table 1. Computation time vs mission time.

Scenario	Computation Time (s)	Mission Time (s)
Figure 3	< 5	≈ 165
Figure 4	< 8	≈ 280
Figure 6a	< 4	≈ 135
Figure 6b	< 6	≈ 200
Figure 6c	< 5	≈ 165

V. CONCLUSION

The paper proposed a guidance algorithm for multiple pursuers tasked to execute a synchronous interdiction of a non-maneuvering moving target in an angle-constrained approach. The computer simulation results prove that the proposed simple yet efficient guidance algorithm taking care of final time and terminal angle simultaneously could be implemented in real time. Future research involve including an inter-pursuer collision avoidance capability and transitioning to flight testing the developed algorithms using the fleet of UAVs available at the Naval Postgraduate School.

ACKNOWLEDGEMENTS

The authors would like to thank the Consortium for Robotics and Unmanned Systems Education and Research at the Naval Postgraduate School for funding this research.

REFERENCES

[1] J.A. Winnefeld, and F. Kendall, "Unmanned Systems Integrated Roadmap: FY 2011-2036", USA DoD Report, Reference Number – 11-S-3613, 2011.

[2] D. Smalley, "The Future Is Now: Navy's Autonomous Swarmboats Can Overwhelm Adversaries", https://www.onr.navy.mil/Media-Center/Press-Releases/2014/autonomous-swarm-boat-unmanned-caracas.aspx (accessed February 23, 2017).

[3] M. Kim, and K.V. Grider, "Terminal Guidance for Impact Attitude Angle Constrained Flight Trajectories," IEEE Trans. Aerospace and Electronic Systems, Vol. AES-9, No. 6, Dec. 1973, pp. 852–859.

[4] E.J. Ohlmeyer, "Control of Terminal Engagement Geometry Using Generalized Vector Explicit Guidance," Proc. American Control Conference, IEEE Publ., Piscataway, NJ, June 2003, pp. 396–401.

[5] C.K. Ryoo, H. Cho, and M.J. Tahk, "Time-to-Go Weighted Optimal Guidance with Impact Angle Constraints," IEEE Trans. Control Systems Technology, Vol. 14, No. 3, May 2006, pp. 483–492.

[6] G.A. Harrison, "Hybrid Guidance Law for Approach Angle and Time-of-Arrival Control," Journal of Guidance, Control, and Dynamics, Vol. 35, No. 4, July–Aug. 2012, pp. 1104–1114.

[7] V. Shaferman, and T. Shima, "Linear Quadratic Guidance Laws for Imposing a Terminal Intercept Angle," Journal of Guidance, Control, and Dynamics, Vol. 31, No. 5, Sept.–Oct. 2008, pp. 1400–1412.

[8] R. Bardhan, and D. Ghose, "Nonlinear Differential Games-Based Impact-Angle-Constrained Guidance," Journal of Guidance, Control, and Dynamics, Vol. 38, No. 3, 2015, pp. 384–402.

[9] C.K. Ryoo, A. Tsourdos, and B. White, "Optimal Impact Angle Control Guidance Law Based on Linearization About Collision Triangle," Journal of Guidance, Control, and Dynamics, Vol. 37, No. 3, May–June 2014, pp. 958–964.

[10] T. Shima, "Intercept-Angle Guidance," Journal of Guidance, Control, and Dynamics, Vol. 34, No. 2, March–April 2011, pp. 484–492.

[11] S.R. Kumar, S. Rao, and D. Ghose, "Nonsingular Terminal Sliding Mode Guidance with Impact Angle Constraints," Journal of Guidance, Control, and Dynamics, Vol. 37, No. 4, July–Aug. 2014, pp. 1114–1130.

[12] S. Rao, and D. Ghose, "Terminal Impact Angle Constrained Guidance Laws Using Variable Structure Systems Theory," IEEE Transactions on Control Systems Technology, Vol. 21, No. 6, Nov. 2013, pp. 2350–2359.

[13] B.S. Kim, J.G. Lee, and H.S. Han, "Biased PNG Law for Impact with Angular Constraint," IEEE Transactions on Aerospace and Electronic Systems, Vol. 34, No. 1, Jan. 1998, pp. 277–288.

[14] A. Ratnoo, and Ghose, D., "Impact Angle Constrained Interception of Stationary Targets," Journal of Guidance, Control, and Dynamics, Vol. 31, No. 6, Nov.–Dec. 2008, pp. 1817–1822.

[15] A. Ratnoo, and D. Ghose, "Impact Angle Constrained Guidance Against Nonstationary Nonmaneuvering Targets," Journal of Guidance, Control, and Dynamics, Vol. 33, No. 1, Jan.–Feb., 2010, pp. 269–275.

[16] C.H. Lee, T.H. Kim, and M.J. Tahk, "Interception Angle Control Guidance Using Proportional Navigation with Error Feedback," Journal of Guidance, Control, and Dynamics, Vol. 36, No. 5, Sept. 2013, pp. 1556–1561.

[17] S. Ghosh, D. Ghose, and S. Raha, "Composite Guidance for Impact Angle Control Against Higher Speed Targets," Journal of Guidance, Control, and Dynamics, Vol. 39, No, 1, Jan.–Feb. 2016, pp. 98–117.

[18] M.G. Yoon, "Relative Circular Navigation Guidance for the Impact Angle Control Problem," IEEE Transactions on Aerospace and Electronic Systems, Vol. 44, No. 4, Oct. 2008, pp. 1449–1463.

[19] I.S. Jeon, J.I. Lee, and M.J. Tahk, "Impact-Time-Control Guidance Law for Anti-Ship Missiles," IEEE Transactions on Control Systems Technology, Vol. 14, No. 2, March 2006, pp. 260–266.

[20] J.I. Lee, I.S. Jeon, and M.J. Tahk, "Guidance Law to Control Impact Time and Angle," IEEE Aerospace and Electronic Systems Magazine, Vol. 43, No. 1, Jan. 2007, pp. 301–310.

[21] I.S. Jeon, J.I. Lee, and M.J. Tahk, "Homing Guidance Law for Cooperative Attack of Multiple Missiles," Journal of Guidance, Control, and Dynamics, Vol. 33, No. 1, pp. 275–280, Jan.–Feb. 2010.

[22] S. Ghosh, D. Ghose, and S. Raha, "Three Dimensional Retro-PN Based Impact Time Control for Higher Speed Nonmaneuvering Targets," Proceedings of IEEE Conference on Decision and Control, IEEE Publ., Piscataway, NJ, Dec. 2013, pp. 4865–4870.

[23] S.R. Kumar, and D. Ghose, "Impact Time and Angle Control Guidance", Proc. AIAA Guidance, Navigation, and Control Conference, AIAA SciTech Forum, (AIAA 2015-0616), 2015.

[24] S.Ghosh, O.A. Yakimenko, D.T. Davis, and T.H. Chung, "Unmanned Aerial Vehicle Guidance for an All-Aspect Approach to a Stationary Point," Accepted for publication in Journal of Guidance, Control, and Dynamics

[25] N. Dhananjay, and D. Ghose, "Accurate time-to-go estimation for proportional navigation guidance", Journal of Guidance, Control, and Dynamics, Vol. 37, No, 4, July-Aug 2014, pp. 1378–1383.

[26] N.A. Shneydor, "Missile Guidance and Pursuit – Kinematics, Dynamics and Control", Hardwood Publishing, 1998, pp. 101-105.

[27] S. Ghosh, D. Ghose, and S. Raha, "Unified Time-To-Go Algorithms for Proportional Navigation Class of Guidance," Journal of Guidance, Control, and Dynamics, Vol. 39, No, 6, June 2016, pp. 1188–1205.